Identifying the Lipid–Protein Interface and Transmembrane Structural Transitions of the Torpedo Na,K-ATPase Using Hydrophobic Photoreactive Probes †

ARTICLE *in* BIOCHEMISTRY · DECEMBER 2000

Impact Factor: 3.02 · DOI: 10.1021/bi0015461 · Source: PubMed

2 AUTHORS, INCLUDING:

ed Mccardy
Texas Tech University Health Sciences Center
10 PUBLICATIONS **275** CITATIONS

SEE PROFILE

Identifying the Lipid−Protein Interface and Transmembrane Structural Transitions of the *Torpedo* Na,K-ATPase Using Hydrophobic Photoreactive Probes†

Michael P. Blanton* and Elizabeth A. McCardy

Departments of Pharmacology and Anesthesiology, Texas Tech University Health Sciences Center, Lubbock, Texas 79430

Received July 5, 2000; Revised Manuscript Received August 15, 2000

ABSTRACT: To identify regions of the *Torpedo* Na,K-ATPase α-subunit that interact with membrane lipid and to characterize conformationally dependent structural changes in the transmembrane domain, we have proteolytically mapped the sites of photoincorporation of the hydrophobic compounds 3-(trifluoromethyl)-3-(*m*-[^{125}I]iodophenyl)diazirine ([^{125}I]TID) and the phosphatidylcholine analogue [^{125}I]TIDPC/16. The principal sites of [^{125}I]TIDPC/16 labeling were identified by amino-terminal sequence analysis of proteolytic fragments of the Na,K-ATPase α-subunit and are localized to hydrophobic segments M1, M3, M9, and M10. These membrane-spanning segments have the greatest levels of exposure to the lipid bilayer and constitute the bulk of the lipid−protein interface of the Na,K-ATPase α-subunit. The extent of [^{125}I]TID and [^{125}I]TIDPC/16 photoincorporation into these transmembrane segments was the same in the E_1 and E_2 conformations, indicating that lipid-exposed segments located at the periphery of the transmembrane complex do not undergo large-scale movements during the cation transport cycle. In contrast, for [^{125}I]-TID but not for [^{125}I]TIDPC/16, there was enhanced photoincorporation in the E_2 conformation, and this component of labeling mapped to transmembrane segments M5 and M6. Conformationally sensitive [^{125}I]-TID photoincorporation into the M5 and M6 segments does not reflect a change in the levels of exposure of these segments to the lipid bilayer as evidenced by the lack of [^{125}I]TIDPC/16 labeling of these two segments in either conformation. These results suggest that [^{125}I]TID promises to be a useful tool for structural characterization of the cation translocation pathway and for conformationally dependent changes in the pathway. A model of the spatial organization of the transmembrane segments of the Na,K-ATPase α- and β-subunits is presented.

The Na,K-ATPase[1] is a transmembrane protein that uses the energy derived from the hydrolysis of adenosine triphosphate (ATP) to transport sodium and potassium ions across the plasma membrane, thereby creating an electrochemical gradient (*1*). The enzyme is comprised of a catalytic α-subunit (112 kDa) which contains the site of phosphorylation and cation transport sites and a smaller glycosylated β-subunit (∼40−60 kDa). The Na,K-ATPase α-subunit is structurally similar to the catalytic subunit from other members of the family of P-type ion-motive ATPases, such as the sarcoplasmic reticulum Ca^{2+}-ATPase and the H^+-ATPase (recent reviews include refs *2*−*4*). Hydropathy plots are consistent with each α-subunit containing 10 membrane-spanning segments, and a variety of studies have further defined the topological organization (*5*). Three-dimensional structures for the Ca^{2+}-ATPase (2.6 Å resolution) and H^+-ATPase (8 Å resolution) have recently been reported and confirm the presence of 10 transmembrane α-helices in each α-subunit (*6*, *7*). While the three-dimensional structure of the Na,K-ATPase is less well defined (*8*), a variety of experimental approaches have resulted in tentative models of the spatial organization of transmembrane segments (*9*). Proteolysis experiments have demonstrated that the cation binding (occlusion) sites are located within the transmembrane domain (*10*, *11*), and biochemical and molecular biological studies have implicated amino acids within transmembrane segments M4−M6 and M8 as being involved in cation occlusion (ref *12* and references therein). For the Ca^{2+}-ATPase, two calcium binding sites formed by residues contained within each of these transmembrane segments have been described and a pathway for Ca^{2+} has been proposed (*6*). While the high-resolution structure of the Ca^{2+}-ATPase has provided tremendous insight into the structure and function of the Ca^{2+}-ATPase and P-type ion-motive ATPases in general, it is also evident that a detailed mechanistic appreciation of the molecular events that underlie cation transport will require a more complete understanding of the structure of the cation translocation pathway as well as the structural changes that occur in the transmembrane domain during the ion transport cycle. It also remains to be

† This research was supported in part by American Heart Association Texas Affiliate Grant-In-Aid 9950783Y.

* To whom correspondence should be addressed: Department of Pharmacology, Texas Tech University Health Sciences Center, 3601 4th St., Lubbock, TX 79430. Telephone: (806) 743-2425. Fax: (806) 743-2744. E-mail: phrmpb@ttuhsc.edu.

[1] Abbreviations: Na,K-ATPase, sodium- and potassium-transporting adenosine triphosphate hydrolase; AChR, nicotinic acetylcholine receptor; [^{125}I]TID, 3-(trifluoromethyl)-3-(*m*-[^{125}I]iodophenyl)diazirine; TTDPC/16, 1-*O*-hexadecanoyl-2-*O*-[9-[[[2-(tributylstannyl)-4-(trifluoromethyl-3*H*-diazirin-3-yl)benzyl]oxy]carbonyl]nonanoyl]-*sn*-glycero-3-phosphocholine; CDTA, 1,2-cyclohexanediaminetetraacetic acid; ATPase buffer, 30 mM histidine and 1 mM CDTA (pH 7.4) with either 30 mM NaCl or 30 mM KCl; SDS, sodium dodecyl sulfate; PAGE, polyacrylamide gel electrophoresis; Tricine, β-[2-hydroxy-1,1-bis-(hydroxymethyl)ethyl]glycine; HPLC, high-performance liquid chromatography.

10.1021/bi0015461 CCC: $19.00
Published on Web 10/07/2000

established whether the other P-type ion-motive ATPases, including the Na,K-ATPase, have the same spatial organization of transmembrane segments and the degree to which the structures of the cation binding sites are homologous.

In this report, we have employed the hydrophobic photoreactive compounds 3-(trifluoromethyl)-3-(*m*-[^{125}I]iodophenyl)diazirine ([^{125}I]TID) and the phosphatidylcholine analogue [^{125}I]TIDPC/16 to allow us to identify which membrane-spanning segments in the α-subunit of the *Torpedo* Na,K-ATPase face the lipid bilayer. Identification of lipid-exposed transmembrane segments will provide definition of the lipid−protein interface of the Na,K-ATPase α-subunit and further distinguish the spatial organization of membrane-spanning segments. By photolabeling the Na,K-ATPase under conditions which stabilize two different conformations and then characterizing the sites of labeling, we may also detect movements of the transmembrane segments that occur during ion transport.

We report that N-terminal sequence analysis of purified proteolytic fragments establishes that the principal sites of [^{125}I]TIDPC/16 labeling are localized to transmembrane segments M1, M3, M9, and M10. These segments then constitute the bulk of the lipid−protein interface of the Na,K-ATPase α-subunit. The extent of [^{125}I]TIDPC/16 photoincorporation into these transmembrane segments is unaffected by conformational transitions of the Na,K-ATPase, indicating that lipid-exposed segments which are located at the periphery of the transmembrane complex do not undergo large-scale movements during the ion transport cycle. In contrast, there is conformationally sensitive [^{125}I]TID photoincorporation into transmembrane segments M5 and M6. These segments are not in contact with lipid as evidenced by a lack of [^{125}I]TIDPC/16 labeling, suggesting that [^{125}I]TID is binding within the cation translocation pathway and reporting conformationally dependent structural changes in the pathway. The results presented here begin to define the spatial organization of transmembrane segments in the Na,K-ATPase and suggest that [^{125}I]TID provides a useful tool for examining the structure of the cation translocation pathway and transport-linked structural transitions.

EXPERIMENTAL PROCEDURES

Materials. [^{125}I]TID (∼10 Ci/mmol) was purchased from Amersham and stored in 75% ethanol at 4 °C. [^{125}I]TIDPC/16 was prepared by by radioiododestanylation of the tin-based precursor 1-*O*-hexadecanoyl-2-*O*-[9-[[[2-(tributylstannyl)-4-(trifluoromethyl-3*H*-diazirin-3-yl)benzyl]oxy]-carbonyl]nonanoyl]-*sn*-glycero-3-phosphocholine (TTDPC/16) and stored in an ethanol/toulene mixture (1:1) at 4 °C (*13*). The tin-based precursor (TTDPC/16) was a generous gift from J. Brunner of the Swiss Federal Institute of Technology (ETH, Zurich, Switzerland). Histidine, NaCl, KCl, 1,2-cyclohexanediaminetetraacetic acid (CDTA), and other general use biochemicals as well as ouabain were purchased from Sigma. L-1-Tosylamido-2-phenylethyl chloromethyl ketone-treated trypsin was from Worthington Biochemical Corporation, *Staphylococcus aureus* V8 protease from ICN, and Genapol C-100 (10%) from Calbiochem. Prestained low-molecular weight gel standards were purchased from Life Technologies, Inc.

Na,K-ATPase Preparation. Na,K-ATPase-containing membranes were prepared from the electric organ of the marine elasmobranch *Torpedo californica*. Procedures used for the isolation of nicotinic acetylcholine receptor (AChR) rich postsynaptic membranes from the *Torpedo* electric organ (*14*, *15*) yield a preparation that is also very rich in Na,K-ATPase protein. For these studies, sucrose density gradient fractions that are rich in Na,K-ATPase, as judged by SDS−PAGE, were pooled (the Na,K-ATPase typically represents ∼45% of the total protein). *Torpedo* Na,K-ATPase membranes in ∼36% sucrose and 0.02% sodium azide were stored at −80 °C. The Na,K-ATPase activity was determined as described previously (*16*) and was the difference between the extent of ATP hydrolysis measured in the presence and absence of 3 mM ouabain. The ATPase enzyme used in these studies had a specific activity of 21 μmol of P_i released mg^{-1} min^{-1} at 25 °C. The protein was quantified by the method of Lowry et al. (*17*) using bovine serum albumin as a standard.

Photolabeling of Na,K-ATPase Membranes with [^{125}I]TID and [^{125}I]TIDPC/16. For analytical labeling experiments, *Torpedo* Na,K-ATPase membranes (1 mg) in ∼36% sucrose and 0.02% sodium azide were diluted 10-fold by addition of distilled water and pelleted by centrifugation (39000*g* for 1 h). The membrane pellet was then resuspended in a small volume (0.2 mL) of ATPase buffer [30 mM histidine and 1 mM CDTA (pH 7.4)] and [^{125}I]TID or [^{125}I]TIDPC/16 added (total ethanol concentration of <1%). After mixing, the membranes were divided into two equal volumes (0.1 mL) and each diluted up to 1 mL with ATPase buffer containing either 30 mM NaCl or 30 mM KCl (final concentrations, 0.5 mg/mL protein and ∼0.4 μM [^{125}I]TID or [^{125}I]TIDPC/16). These conditions are known to stabilize either the E_1 (30 mM NaCl) or E_2 (30 mM KCl) conformation of the Na,K-ATPase (*18*). After a 2 h incubation at room temperature, the samples were then irradiated with a 365 nm UV lamp (Spectroline EN-280L) for 7 min at a distance of less than 1 cm, and centrifuged at 39000*g* for 1 h. Pellets were solubilized in electrophoresis sample buffer and subjected to SDS−PAGE (*19*). Prior to UV irradiation, all operations were performed under reduced light conditions, and membrane incubations were carried out in glass test tubes or vials. Preparative-scale labeling experiments (10 mg of total protein per labeling condition) were conducted in a similar fashion, with appropriate increases in the volumes that were used (typically 125 μCi of [^{125}I]TID was used per labeling condition).

For analytical labeling experiments, 1.0 mm thick SDS−PAGE gels were used (1.5 mm thick for preparative labeling experiments) containing separating gels composed of 8% polyacrylamide and 0.33% bis-acrylamide. Following electrophoresis, gels were stained with Coomassie Blue R-250 to visualize polypeptide bands. Analytical gels were dried and exposed to Kodak X-OMAT LS film with an intensifying screen at −80 °C (exposure for 8−24 h). For gels (preparative and analytical) in which the Na,K-ATPase α-subunit was to be subjected to proteolytic mapping, the 8% acrylamide gels were soaked in distilled water overnight and the Na,K-ATPase α-subunit was excised from the gels. Proteolytic mapping of the sites of [^{125}I]TID and [^{125}I]TIDPC/16 photoincorporation within the Na,K-ATPase α-subunit using *S. aureus* V8 protease was performed according to the method of Cleveland et al. (*20*) and as described in detail by Blanton et al. (*13*). Analytical mapping gels were dried and exposed to Kodak X-OMAT LS film with an intensifying

screen at −80 °C (exposure for 3−7 days). For preparative gels, the [^{125}I]TID- and [^{125}I]TIDPC/16-labeled V8 protease fragments were eluted from the excised gel pieces into 15 mL of elution buffer [0.1 M NH_4HCO_3, 0.1% (w/v) SDS, and 1% β-mercaptoethanol (pH 7.8)] for 4 days at room temperature with gentle mixing. The gel suspensions were then filtered through Whatman No. 1 paper and concentrated to ~350 μL using a Centriprep-10 concentrator (Amicon). For V8 fragments that were to be further enzymatically digested, excess SDS was removed by acetone precipitation (~85% acetone at −20 °C for 12 h).

For analytical labeling experiments, [^{125}I]TID and [^{125}I]-TIDPC/16 photoincorporation into the Na,K-ATPase α-subunit as well as V8 protease cleavage fragments was quantified by cutting out the bands from the dried polyacrylamide gel and determining the amount of ^{125}I counts per minute present in each band by γ-counting in a Packard Cobra II γ-counter (10 min of counting time/band). The relative amounts of protein or peptide were determined by densiometric analysis (Un-Scan-It Software, Silk Scientific Corp.) of stained polyacrylamide gels.

Digestion of [^{125}I]TIDPC/16-Labeled V8 Protease Fragments. To further map the sites of [^{125}I]TIDPC/16 labeling in V8 protease fragments of the Na,K-ATPase α-subunit, fragments V8−25, V8−14, and V8−15 were further enzymatically digested. For digestion with trypsin, acetone-precipitated fragments V8−25 and V8−14 were resuspended in approximately 300 μL of 0.1 M NH_4HCO_3, 0.02% (w/v) SDS, and 0.5% Genapol C-100 (pH 7.8) (1−2 mg/mL protein). Trypsin was added at a 20% (w/w) enzyme-to-substrate ratio and the digestion allowed to proceed for 4−5 days at room temperature. For further digestion with V8 protease, fragment V8−15 was resuspended in approximately 250 μL of 0.1 M NH_4HCO_3 and 0.1% (w/v) SDS (pH 7.8) (1−2 mg/mL protein). V8 protease was added at a 50% (w/w) enzyme-to-substrate ratio and the digestion allowed to proceed for 4−5 days at room temperature. For both tryptic and V8 protease digests, a small aliquot of each sample (25 μL) was electrophoresed on an analytical (1.0 mm thick) 16.5% T/6% C Tricine SDS−PAGE gel (*21*) with at least one reference lane containing prestained low-molecular weight protein standards (Life Technologies, Inc.). The Tricine gel was stained, destained, and dried for autoradiography. The bulk of the proteolytic digests were then submitted to preparative-scale (1.5 mm thick) 16.5% T/6% C Tricine gel analysis. Preparative Tricine gels were stained, destained, and soaked in water overnight. Using the autoradiograph from the analytical Tricine gel in conjunction with the prestained protein standards, [^{125}I]TIDPC/16-labeled fragments were excised from the gel and eluted into 4 mL of elution buffer for 4 days at room temperature.

Reverse-Phase HPLC Purification of [^{125}I]TID- and [^{125}I]-TIDPC/16-Labeled Proteolytic Fragments. Large V8 fragments of the Na,K-ATPase α-subunit labeled with [^{125}I]TID or [^{125}I]TIDPC/16, as well as [^{125}I]TIDPC/16-labeled fragments resulting from further enzymatic digestions, were further purified by reverse-phase HPLC. A Brownlee Aquapore C_4 column (100 mm × 2.1 mm) was employed with a binary elution gradient comprised of solvent A (0.08% trifluoroactetic acid in water) and solvent B (0.05% trifluoroacetic acid in 60% acetonitrile/40% 2-propanol). A nonlinear elution gradient was employed (25 to 100% solvent B over the course of 80 min), and the elution of peptides was monitored by the absorbance at 210 nm. Collected fractions were assessed for radioactivity, and the peak protein/radioactivity-containing fractions were pooled, dried by vacuum centrifugation, and resuspended in 20 μL of 0.1 M NH_4HCO_3 and 0.1% (w/v) SDS (pH 7.8) for protein sequence analysis.

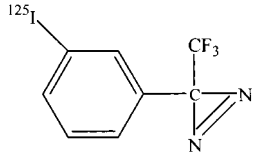

FIGURE 1: Chemical structure of 3-(trifluoromethyl)-3-(*m*-[^{125}I]-iodophenyl)diazirine ([^{125}I]TID).

Sequence Analysis. Amino-terminal sequence analysis was performed on a Beckman Instruments (Porton) model 20/20 protein sequencer using gas-phase cycles (Texas Tech University Biotechnology Core Facility, Lubbock, TX). Peptide aliquots (25 μL) were immobilized on chemically modified glass fiber disks (Beckman Instruments), which were used to improve the sequencing yields of hydrophobic peptides. Each peptide was subjected to 5−10 cycles of sequencing (automated Edman degradation).

RESULTS

Characterization of [^{125}I]TID Photoincorporation into the Torpedo Na,K-ATPase. Initial photolabeling experiments were designed to characterize the general pattern and conformational sensitivity of [^{125}I]TID (Figure 1) photoincorporation into the *Torpedo* Na,K-ATPase. Na,K-ATPase membranes were equilibrated with [^{125}I]TID (0.4 μM) under conditions which stabilize either the E_1 (30 mM Na^+ buffer) or E_2 (30 mM K^+ buffer) conformation (*18*). After a 2 h incubation, membranes were exposed to UV light (365 nm) for 7 min and then pelleted by centrifugation. Membrane pellets were solubilized in electrophoresis sample buffer, and the extent of photoincorporation into the Na,K-ATPase was monitored by SDS−PAGE followed by autoradiography. The autoradiograph of an 8% polyacrylamide slab gel (Figure 2) reveals that there is substantial [^{125}I]TID photoincorporation into the Na,K-ATPase α-subunit (α_{NK}) as well as into each subunit of the nicotinic acetylcholine receptor (AChR, α, β, γ, and δ). The Na,K-ATPase α-subunit and AChR subunits represent 44 and 36% of the total protein, respectively, contained within the *Torpedo* membrane preparation as determined by densiometric analysis of stained 8% acrylamide gels. [^{125}I]TID photoincorporation into each of the subunits of the AChR has been extensively characterized, thereby providing an internal control for these photolabeling experiments (*22*−*26*). [^{125}I]TID also photoincorporates into the β-subunit of the Na,K-ATPase, including the *Torpedo* β-subunit (*25*, *27*, *28*). However, in the *Torpedo* AChR-rich membrane preparations used in this study, [^{125}I]TID photoincorporation into the Na,K-ATPase β-subunit is obscured by the heavy labeling of the AChR γ- and δ-subunits (*24*, *25*). As is evident in the autoradiograph shown in Figure 2, there is a small but clearly discernible increase in the extent of [^{125}I]TID photoincorporation into the Na,K-ATPase α-subunit in the E_2 (K^+ lane) versus the E_1 (Na^+ lane) conformation. On the basis of γ-counting of excised gel

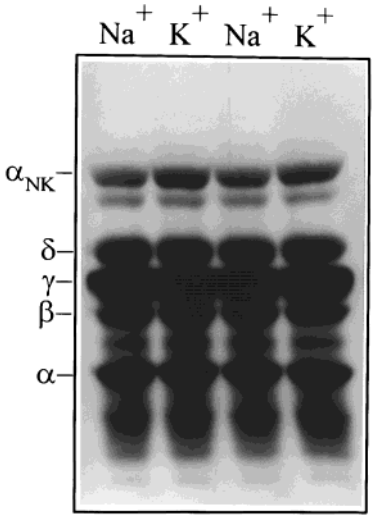

FIGURE 2: [^{125}I]TID photoincorporation into the *Torpedo* Na,K-ATPase in the E_1 and E_2 conformations. Na,K-ATPase-containing membranes isolated from the electric organ of the marine elasmobranch *T. californica* were equilibrated (2 h) with [^{125}I]TID (0.4 μM) under conditions which stabilize either the E_1 [30 mM histidine and 1 mM CDTA (pH 7.4) with 30 mM NaCl] or E_2 conformation of the Na,K-ATPase [30 mM histidine and 1 mM CDTA (pH 7.4) with 30 mM KCl] (*18*). Following a 2 h incubation, membranes were irradiated at 365 nm (Spectroline EN-280L) for 7 min (at a distance of <1 cm) and the membranes pelleted by centrifugation. Membrane polypeptides were resolved by SDS−PAGE (1.0 mm thick, 8% polyacrylamide gel), visualized by Coomassie Blue R-250 staining, and subjected to autoradiography (exposure for 16 h with an intensifying screen). Labeled lipid and free photolysis products were electrophoresed from the gel with the tracking dye. In addition to the substantial [^{125}I]TID incorporation into the subunits of the nicotinic acetylcholine receptor (AChR, α, β, γ, and δ), there is also significant labeling of the α-subunit of the Na,K-ATPase (α_{NK}). The extent of [^{125}I]TID photoincorporation into the Na,K-ATPase α-subunit labeled in the E_1 and E_2 states is shown in the Na^+ and K^+ lanes, respectively. Labeling of the β-subunit of the Na,K-ATPase is obscured by the AChR γ- and δ-subunits (*24*), and the [^{125}I]TID-labeled band migrating with an electrophoretic mobility slightly faster than that of α_{NK} is the CLC-0 voltage-gated chloride channel (*13*).

bands, ~1% of the α-subunits incorporated ^{125}I and there is a 28.8 ± 3.1% increase in the extent of [^{125}I]TID photoincorporation into the Na,K-ATPase α-subunit in the E_2 versus the E_1 conformation ($n = 8$). In each of these analytical [^{125}I]-TID photolabeling experiments, densiometric analysis of stained 8% acrylamide gels reveals that there is no significant difference (>7%) in the amount of α-subunit protein present under each of the two labeling conditions. An earlier [^{125}I]-TID study by Modyanov and colleagues (*28*) resulted in a nearly identical increase in the extent of photoincorporation into the α-subunit in the E_2 conformation, with no detectable difference in the extent of labeling in the β-subunit.

[^{125}I]TID photoincorporation within the Na,K-ATPase α-subunit was next mapped by limited enzymatic digestion with *S. aureus* V8 protease (*13*, *20*). Inspection of the autoradiograph of a 15% acrylamide mapping gel containing the V8 protease digests of the Na,K-ATPase α-subunit labeled with [^{125}I]TID in the E_1 and E_2 conformations (Figure 3) reveals significant photoincorporation into several fragments. On the basis of the apparent molecular mass of each labeled fragment, the principal [^{125}I]TID-labeled fragments were designated V8−25 (25 kDa), V8−15 (15 kDa), V8−14 (14 kDa), V8−12 (12 kDa), and V8−4 (4 kDa). Close

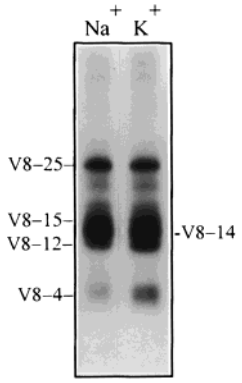

FIGURE 3: Proteolytic mapping of the sites of [^{125}I]TID photoincorporation into the α-subunit of the *Torpedo* Na,K-ATPase using *S. aureus* V8 protease. Na,K-ATPase membranes were labeled with [^{125}I]TID under conditions which stabilize either the E_1 (Na^+) or E_2 (K^+) conformation (see the legend of Figure 2) and subjected to SDS−PAGE on a 1.0 mm thick 8% polyacrylamide gel. The Na,K-ATPase α-subunit bands were excised following identification by staining, transferred to the wells of a 15% acrylamide mapping gel, and overlaid with 6 μg of *S. aureus* V8 protease (see Experimental Procedures). The Na,K-ATPase α-subunit was proteolytically digested as it migrated through the 4.5% acrylamide stacking gel (constant voltage of 50 V, transit time of ~3 h), and the resulting fragments were then resolved on the lower 15% acrylamide separating gel. Following electrophoresis, the mapping gel was stained with Coomassie Blue R-250 and subjected to autoradiography (exposure for 1−2 weeks with an intensifying screen). The principal [^{125}I]TID-labeled proteolytic fragments are in accordance with their apparent molecular masses: V8−25, 25 kDa; V8−15, 15 kDa; V8−14, 14 kDa; V8−12, 12 kDa; and V8−4, 4 kDa.

inspection of the autoradiograph in Figure 3 reveals that two of the V8 protease fragments, V8−12 and V8−4, exhibit enhanced [^{125}I]TID photoincorporation in the E_2 (K^+ lane) versus the E_1 (Na^+ lane) conformation. Direct counting of the excised gel bands shows that for V8 fragments V8−12 and V8−4 there are (1.72 ± 0.13)- and (1.8 ± 0.2)-fold increases in the extent of [^{125}I]TID photoincorporation in the E_2 conformation, respectively ($n = 6$). In contrast, no statistically significant difference (>5%) was found in the extent of [^{125}I]TID photoincorporation in any of the other V8 protease fragments isolated from ATPase labeled in the two different conformations. Furthermore, densiometric analysis of the stained 15% acrylamide mapping gels revealed that in each case there was a less than 10% difference in the amount of peptide present for each V8 fragment isolated from ATPase labeled in the two different conformations.[2] From a preparative-scale labeling experiment (10 mg per labeling condition), each of the principal [^{125}I]-TID-labeled V8 fragments was isolated (^{125}I counts per minute recoveries were typically >90%) and further purified by reverse-phase HPLC. The HPLC elution profiles of the [^{125}I]TID-labeled V8 fragments (Figure 4) show that for each fragment and for each labeling condition (E_1 vs E_2 conformation) there is a primary peak of ^{125}I counts per minute and a corresponding peak of protein absorbance (HPLC column ^{125}I counts per minute recoveries were typically >80%). The pool of peak ^{125}I counts per minute-containing

[2] For the Na,K-ATPase labeled with [^{125}I]TID in the absence of cations, a condition known to stabilize the E_2 conformation (*32*), the extent of photoincorporation into the intact α-subunit and the pattern and extent of incorporation into V8 protease fragments were identical to those determined in the presence of 30 mM K^+ (E_2 conformation).

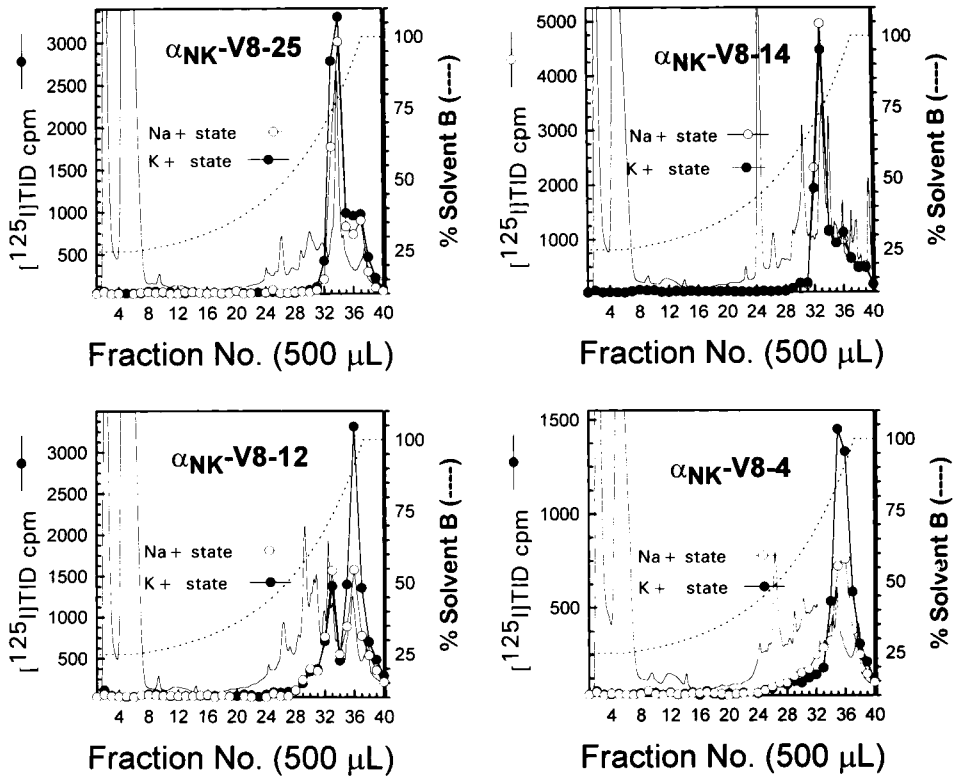

FIGURE 4: Reverse-phase HPLC purification of [^{125}I]TID-labeled V8 protease fragments of the Na,K-ATPase α-subunit. [^{125}I]TID-labeled proteolytic fragments were isolated from *S. aureus* V8 protease digests of the α-subunit of the Na,K-ATPase labeled in the E_1 (Na^+) and E_2 (K^+) conformations (see Figure 3). The [^{125}I]TID-labeled fragments were further purified by reverse-phase HPLC on a Brownlee Aquapore C_4 column (100 mm × 2.1 mm) as described in Experimental Procedures. The elution of peptides was monitored by absorbance at 210 nm (solid line, not indicated on axis) and elution of ^{125}I by γ-counting of each 500 μL fraction (● and ○). The HPLC elution profile for fragments isolated from the Na,K-ATPase labeled with [^{125}I]TID in the E_1 (○) or E_2 (●) state are shown for fragments V8−25, V8−14, V8−12, and V8−4.

Table 1: Identification of [^{125}I]TID-Labeled Fragments Produced by *S. aureus* V8 Protease Digestion of the Na,K-ATPase α-Subunit[a]

fragment	apparent molecular mass (kDa)	N-terminal sequence (pmol of residue/cycle)	starting residue	predicted carboxy terminus (transmembrane segments)
V8−25	25	S(460)D(209)I(406)M(450)K(314)	S^{828}	Y^{1022} (M7−M10)
V8−15A	15	V(60)S(24)L(47)D(50)D(40)	V^{39}	E^{176} (M1 and M2)
V8−15B	15	Y(482)S(154)S(135)E(242)N(205)	Y^{231}	E^{365} (M3 and M4)
V8−14	14	Y(94)T(75)C(22)H(47)T(48)	Y^{915}	Y^{1022} (M8−M10)
V8−12	12	G(383)C(288)Q(88)R(131)Q(88)	G^{703}	E^{824} (M5 and M6)
V8−4	4	G(125)R(129)L(152)I(149)F(112)	G^{764}	E^{824} (M5 and M6)

[a] Apparent molecular mass values are those estimated from the electrophoretic mobility on 15% acrylamide mapping gels (Figure 3). For the V8−15 fragment, two peaks of ^{125}I counts per minute were evident in the reverse-phase HPLC profile. HPLC fractions 35−37 were pooled for V8−15A and fractions 38−40 for V8−15B. The sequence of each fragment was identified within the primary structure of the *T. californica* Na,K-ATPase α-subunit (*29*). Sequencing yields are presented for V8 fragments isolated from the Na,K-ATPase labeled with [^{125}I]TID under conditions which stabilize the E_2 conformation; identical sequences and similar yields were obtained for fragments isolated from ATPase labeled in the E_1 conformation.

fractions for fragments V8−12 (*35*−*37*) and V8−4 (*35*, *36*) indicate that there are approximately twice as many counts in the fragments isolated from ATPase labeled in the presence of potassium (E_2 conformation) than in the fragments isolated in the presence of sodium (E_1 conformation) [V8−12, Na^+ state, 2350 cpm; K^+ state, 4671 cpm (1.98-fold difference); V8−4, Na^+ state, 1481 cpm; K^+ state, 2780 cpm (1.87-fold difference)]. In contrast, for the pool of peak ^{125}I counts per minute-containing HPLC fractions for V8−25 (*33*−*35*), V8−15 (HPLC profile not shown, peak A, 35−37; peak B, 38−40), and V8−14 (*32*−*34*), there was no significant difference in the total counts for each fragment isolated from ATPase labeled in the two different conformations. For each V8 fragment, the pool of peak ^{125}I counts per minute-containing HPLC fractions was subjected to automated N-terminal amino acid sequence analysis. The first 5−10 amino acids were determined for each V8 fragment with the identity and yield for the first five residues presented in Table 1. For each fragment, a single peptide was detected with any secondary sequences present in an at least 10-fold lower abundance. From the first five residues of each V8 fragment, the amino terminus of each fragment was aligned with the primary structure of the *Torpedo* Na,K-ATPase α-subunit (*29*; Table 1). On the basis of the apparent molecular mass of each fragment estimated from its electrophoretic mobility on a 15% acrylamide mapping gel (Figure 3) and the cleavage specificity of *S. aureus* V8 protease, the carboxy terminus of each fragment was predicted (Table 1). A map

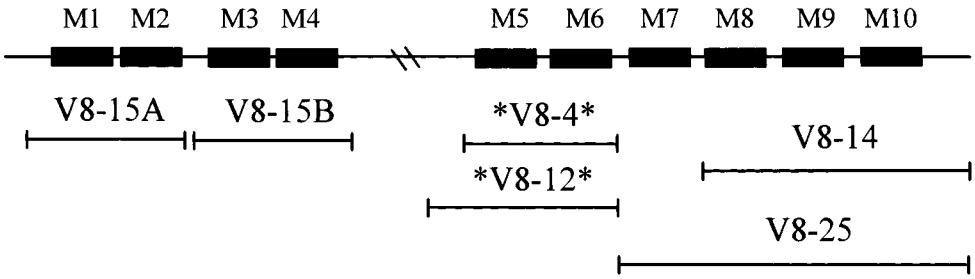

FIGURE 5: Map of [^{125}I]TID-labeled V8 protease fragments in relation to the *Torpedo* Na,K-ATPase α-subunit sequence. The HPLC-purified [^{125}I]TID-labeled V8 protease fragments of the Na,K-ATPase α-subunit (Figure 4) were subjected to automated N-terminal protein sequencing (Edman degradation). Using the amino acids detected in the first 5−10 cycles of Edman degradation, the position of each fragment in relation to the primary structure of the intact *T. californica* Na,K-ATPase α-subunit (*29*) was determined (Table 1). On the basis of the apparent molecular mass of each fragment and the known cleavage specificity of *S. aureus* V8 protease (carboxy-terminal side of glutamic acid and aspartic acid residues), the carboxy terminus of each fragment was predicted. The approximate location of each of the membrane-spanning domains (M1−M10) of the Na,K-ATPase α-subunit are shown, while the large cytoplasmic loop between M4 and M5 has been abbreviated (-\\-). The amino acid stretch and transmembrane segments contained within each V8 fragment are marked with brackets, and fragments V8−12 and V8−4, which exhibited conformationally sensitive [^{125}I]TID labeling, are further denoted with asterisks.

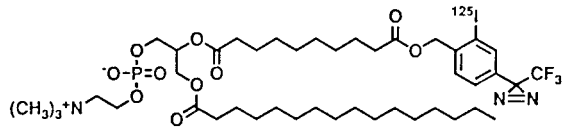

FIGURE 6: Chemical structure of [^{125}I]TIDPC/16.

of the confines of each [^{125}I]TID-labeled V8 fragment within the Na,K-ATPase α-subunit sequence is shown in Figure 5. As is illustrated in the map, the two V8 fragments which exhibited conformationally sensitive [^{125}I]TID photoincorporation, V8−12 and V8−4, are overlapping fragments with each fragment containing almost exclusively membrane-spanning segments M5 and M6. There was no detectable difference in the extent of [^{125}I]TID photoincorporation into V8 fragments V8−25, V8−15, and V8−14, and collectively, these fragments contain transmembrane segments M1−M4 and M7−M10.

From the amount of ^{125}I counts per minute and the intial yield determined from sequence analysis, the specific activities for each fragment were calculated: V8−25, Na^+ condition, 14.6 cpm/pmol, K^+ condition, 15.3 cpm/pmol; V8−15A, Na^+ condition, 5.7 cpm/pmol, K^+ condition, 4.9 cpm/pmol; V8−15B, Na^+ condition, 2.6 cpm/pmol, K^+ condition, 2.9 cpm/pmol; V8−14, Na^+ condition, 13.2 cpm/pmol, K^+ condition, 15.2 cpm/pmol; V8−12, Na^+ condition, 7.8 cpm/pmol, K^+ condition, 15.5 cpm/pmol; and V8−4, Na^+ condition, 10.9 cpm/pmol, K^+ condition, 20.6 cpm/pmol.

Characterization of [^{125}I]TIDPC/16 Photoincorporation into the Na,K-ATPase. In these studies, we sought to extensively map the sites of [^{125}I]TIDPC/16 photoincorporation into the α-subunit of the *Torpedo* Na,K-ATPase. TIDPC/16 (Figure 6) is an analogue of the membrane phospholipid phosphatidylcholine in which the photoreactive (trifluoromethyl)(iodophenyl)diazirine moiety (TID) is located at the end of one of the fatty acyl chains. Photolabeling of the Na,K-ATPase α-subunit with this photoreactive phospholipid was undertaken (1) to determine if the conformationally sensitive [^{125}I]TID photoincorporation into V8 fragments which contain membrane-spanning segments M5 and M6 is a reflection of the increased level of exposure of these segments to the lipid bilayer and (2) to identify the lipid-exposed transmembrane segments of the Na,K-ATPase α-subunit.

As with [^{125}I]TID, initial photolabeling experiments were designed to characterize the general pattern and conformational sensitivity of [^{125}I]TIDPC/16 photoincorporation into the *Torpedo* Na,K-ATPase. Na,K-ATPase membranes were equilibrated with [^{125}I]TIDPC/16 (0.4 μM) under conditions which stabilize either the E_1 (30 mM Na^+ buffer) or E_2 (30 mM K^+ buffer) conformation (*18*) and exposed to UV irradiation and labeled membrane polypeptides identified by SDS−PAGE and autoradiography. The autoradiograph of an 8% polyacrylamide slab gel reveals that in addition to labeling each of the subunits of the AChR, there is substantial [^{125}I]TIDPC/16 photoincorporation into the Na,K-ATPase α-subunit (α_{NK}) (data not shown; see ref *13*). On the basis of γ-counting of excised gel bands, ~1.5% of the α-subunits incorporated ^{125}I and there was no significant difference (>4%) in the extent of [^{125}I]TIDPC/16 photoincorporation into the Na,K-ATPase α-subunit in the E_2 and E_1 conformations ($n = 7$). Nor was there any significant difference (>10%) in the amount of α-subunit protein in the E_2 and E_1 conformations, as revealed by densiometric analysis of the stained 8% polyacrylamide gels.

[^{125}I]TIDPC/16 photoincorporation within the Na,K-ATPase α-subunit was next mapped by limited enzymatic digestion with *S. aureus* V8 protease (*13*, *20*). In Figure 7, autoradiographs of 15% acrylamide mapping gels containing V8 protease digests of the Na,K-ATPase α-subunit labeled with [^{125}I]TID and [^{125}I]TIDPC/16 in the E_1 and E_2 conformation are presented. A side by side inspection of the two autoradiographs reveals that in contrast to [^{125}I]TID there is no apparent difference in the extent of [^{125}I]TIDPC/16 photoincorporation into any of the labeled fragments, and furthermore, there is no detectable [^{125}I]TIDPC/16 incorporation into V8 fragments V8−12 and V8−4. The principal [^{125}I]TIDPC/16-labeled V8 fragments are V8−25, V8−15, and V8−14. From direct counting of gel bands, no significant difference (>10%) was found in the extent of [^{125}I]TIDPC/16 photoincorporation into V8 fragments V8−25, V8−15, and V8−14 isolated from ATPase labeled in the two different conformations. Densiometric analysis of the stained 15% acrylamide mapping gels revealed no significant (>10%) difference in the amount peptide fragment present for each V8 fragment isolated from ATPase labeled in the two different conformations, but did reveal the presence of fragments V8−12 and V8−4. To confirm the identity of the

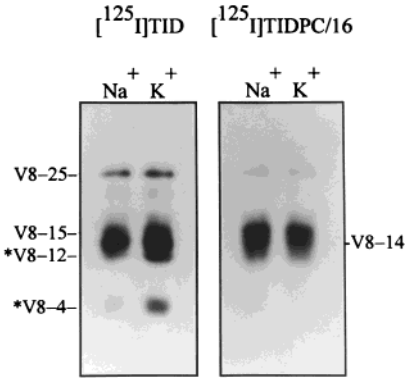

FIGURE 7: Proteolytic mapping of the sites of [^{125}I]TID and [^{125}I]-TIDPC/16 photoincorporation into the α-subunit of the *Torpedo* Na,K-ATPase using *S. aureus* V8 protease. Na,K-ATPase membranes were labeled with [^{125}I]TID or the phospholipid TID analogue [^{125}I]TIDPC/16 under conditions which stabilize either the E_1 (Na^+) or E_2 (K^+) conformation (see the legend of Figure 2) and subjected to SDS−PAGE on 1.0 mm thick 8% polyacrylamide gels. The Na,K-ATPase α-subunit bands were excised following identification by staining, transferred to the wells of 15% mapping gels, and subjected to proteolytic mapping with *S. aureus* V8 protease (see the legend of Figure 3). Following electrophoresis, the mapping gels were stained with Coomassie Blue R-250 and subjected to autoradiography (exposure for 1−2 weeks with an intensifying screen). The principal [^{125}I]TID-labeled proteolytic fragments are as shown in Figure 3: V8−25, V8−15, V8−14, V8−12, and V8−4. [^{125}I]TIDPC/16 photoincorporation is restricted to V8 fragments V8−25, V8−15, and V8−14. The results of N-terminal sequencing of the [^{125}I]TIDPC/16-labeled V8 fragments are presented in Table 2.

principal [^{125}I]TIDPC/16-labeled V8 fragments (V8−25, V8−15, and V8−14), each of these fragments was isolated in a preparative-scale labeling experiment (E_1 conformation only, ^{125}I cpm recoveries were typically >90%) and further purified by reverse-phase HPLC. The HPLC elution profiles of the [^{125}I]TIDPC/16-labeled V8 fragments (data not shown) were nearly identical to those of their [^{125}I]TID-labeled counterparts (Figure 4). As was the case with the [^{125}I]TID-labeled V8 fragments, for each fragment there is a primary peak of ^{125}I counts per minute and a corresponding peak of protein absorbance (HPLC column ^{125}I counts per minute recoveries were typically >80%). For each [^{125}I]TIDPC/16-labeled fragment, peak ^{125}I counts per minute-containing HPLC fractions were pooled {V8−25 (*33*−*36*), V8−14 (*33*−*35*), and V8−15 [peak A (*35*−*37*) and peak B (*39*−*40*)]} and subjected to automated N-terminal amino acid sequence analysis. The first 5−10 amino acids were determined for each V8 fragment with the identity and yield for the first five residues presented in Table 2. For each fragment, a single peptide was detected with any secondary sequences present in an at least 5−10-fold lower abundance. Comparison of the results presented in Tables 1 and 2 confirms that V8 fragments V8−25, V8−15 (A and B), and V8−14 labeled with either [^{125}I]TID or [^{125}I]TIDPC/16 are identical. Therefore, one or more of the transmembrane segments of the Na,K-ATPase α-subunit contained within each of these V8 fragments (M1−M4 and M7−M10; Figure 5) are therefore interpreted as having exposure to the lipid bilayer. In contrast, the lack of [^{125}I]TIDPC/16 labeling of V8 fragments V8−12 (Gly^{703}−Glu^{824}) and V8−4 (Gly^{764}−Glu^{824}) indicates that transmembrane segments M5 and M6 are not in contact with lipid.

From the amount of ^{125}I counts per minute and the intial yield determined from sequence analysis, the specific activities for each fragment were calculated: V8−25, 70 cpm/pmol; V8−15A, 154 cpm/pmol; V8−15B, 25 cpm/pmol; and V8−14, 93 cpm/pmol.

Identifying Individual Lipid-Exposed Rransmembrane Segments of the Na,K-ATPase α-Subunit Using [^{125}I]TIDPC/16. The [^{125}I]TID- and [^{125}I]TIDPC/16-labeled V8 protease fragments (V8−25, V8−15, and V8−14) each contain two or more membrane-spanning segments (Figure 5 and Table 2). Therefore, further mapping studies were conducted to determine which, if not all, of these transmembrane segments are labeled by [^{125}I]TIDPC/16 and hence in contact with lipid. [^{125}I]TIDPC/16-labeled V8 fragments V8−25 and V8−14 (Figure 5 and Table 2) are overlapping fragments and collectively contain transmembrane segments M7−M10. When these two fragments are further enzymatically digested with trypsin and the digests resolved by Tricine SDS−PAGE, for each fragment there are two labeled bands with apparent molecular masses of 3 and 6 kDa that are evident on the corresponding autoradiograph (Figure 8A). These two tryptic fragments, designated T-3 and T-6, were isolated from a Tricine SDS−PAGE gel and further purified by reverse-phase HPLC. For the T-3 fragment isolated from a tryptic digest of either V8−25 or V8−14, two peaks of ^{125}I counts per minute were evident in the HPLC elution profile (Figure 8B). HPLC fractions 33−35 (T-3A) and 37−40 (T-3B) were pooled separately, and each was subjected to protein sequence analysis. For the T-6 fragment, a single peak of ^{125}I counts per minute-containing fractions is evident for both V8−25 and V8−14, and these fractions (*37*−*40*) were pooled and sequenced. Sequence analysis of T-3A and T-3B revealed in each case the presence of a primary peptide beginning at Met^{979} and Asn^{941}, respectively (Table 3). On the basis of the molecular masses of the T-3 fragments and the cleavage specificity of trypsin, the predicted C-termini are Arg^{1004} (T-3A) and Arg^{978} (T-3B), indicating that the two fragments contain transmembrane segments M10 and M9, respectively (Figure 9). Sequence analysis of the T-6 fragment revealed the presence of a peptide beginning at Asn^{941} and a predicted C-terminus at Arg^{1004} (Table 3). As is shown in the map presented in Figure 9, the larger T-6 fragment contains both the M9 and M10 transmembrane segments. The mapping results of the sites of labeling in V8−25 and V8−15 indicate that amino acids within transmembrane segments M9 and M10 have reacted with [^{125}I]-TIDPC/16, and therefore, these segments are exposed to the lipid bilayer (Figure 9). In contrast, the absence of any [^{125}I]-TIDPC/16-labeled fragment(s) containing the M7 and M8 membrane-spanning segments indicates that these segments either are not in contact with lipid or have very limited exposure to the lipid bilayer.

[^{125}I]TIDPC/16-labeled V8 fragment V8−15 (Figure 7) can be resolved into two separate fragments by reverse-phase HPLC, and collectively, the two fragments contain transmembrane segments M1−M4 (Table 2). When these two fragments (unresolved mixture) are further enzymatically digested with V8 protease and the digest is resolved by Tricine SDS−PAGE, the principal [^{125}I]TIDPC/16-labeled fragments migrate with apparent molecular masses of 12, 6, and 4 kDa. Designated V8−12, V8−6, and V8−4, respectively, each of these fragments was further purified by

Table 2: Identification of [^{125}I]TIDPC/16-Labeled Fragments Produced by *S. aureus* V8 Protease Digestion of the Na,K-ATPase α-Subunit[a]

fragment	apparent molecular mass (kDa)	N-terminal sequence (pmol of residue/cycle)	starting residue	predicted carboxy terminus (transmembrane segments)
V8−25	25	S(37)D(27)I(35)M(22)K(31)	S^{828}	Y^{1022} (M7−M10)
V8−15A	15	V(30)S(12.2)L(17.7)D(25)D(16.3)	V^{39}	E^{176} (M1 and M2)
V8−15B	15	Y(44)S(34)S(28)E(31)N(16.1)	Y^{231}	E^{365} (M3 and M4)
V8−14	14 (primary)	Q(23)R(14)K(25)I(26)V(22)	Q^{909}	Y^{1022} (M8−M10)
V8−14	14 (secondary)	Y(14)T(8.4)C(6.2)H(9.7)T(12)	Y^{915}	Y^{1022} (M8−M10)

[a] Apparent molecular mass values are those estimated from the electrophoretic mobility on 15% acrylamide mapping gels (Figure 7). For the V8−15 fragment, two peaks of ^{125}I counts per minute were evident in the reverse-phase HPLC profile. HPLC fractions 35−37 were pooled for V8−15A and fractions 39 and 40 for V8−15B. The sequence of each fragment was identified within the primary structure of the *T. californica* Na,K-ATPase α-subunit (*29*). Sequencing yields are presented for V8 fragments isolated from the Na,K-ATPase labeled with [^{125}I]TIDPC/16 under conditions which stabilize the E_1 conformation.

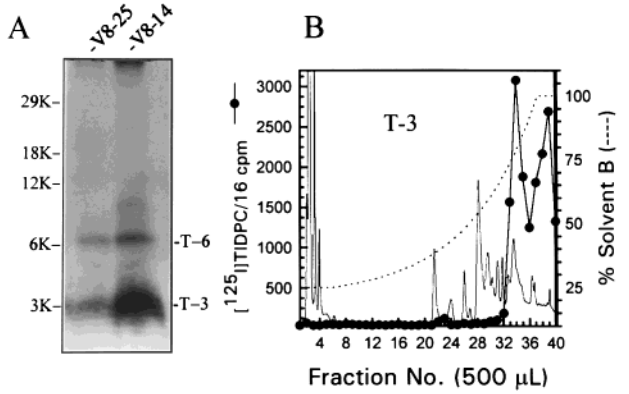

FIGURE 8: Trypsin digestion of Na,K-ATPase V8 protease fragments V8−25 and V8−14 and reverse-phase HPLC purification of the resulting [^{125}I]TIDPC/16-labeled fragments. (A) V8 protease fragments V8−25 and V8−14 (Table 2), isolated from Na,K-ATPase membranes labeled with [^{125}I]TIDPC/16 under conditions which stabilize the E_1 state, were digested with 25% (w/w) trypsin for 4 days. Aliquots of the digests (7.5% of the total) were electrophoresed by Tricine SDS−PAGE and then subjected to autoradiography for 1 week. The migration of prestained molecular mass standards is shown on the right, and the relative molecular masses of the principal [^{125}I]TIDPC/16-labeled digestion products are shown on the left for each V8 fragment. (B) For the tryptic digests of V8−25 and V8−14, the bulk of the material was then electrophoresed on 1.5 mm thick Tricine SDS−PAGE gels, and with the use of prestained molecular mass markers, [^{125}I]TIDPC/16-labeled tryptic fragments T-6 and T-3 were isolated. The [^{125}I]-TID-labeled tryptic fragments were further purified by reverse-phase HPLC on a Brownlee Aquapore C_4 column (100 mm × 2.1 mm) as described in Experimental Procedures. The elution of peptides was monitored by absorbance at 210 nm (solid line, not indicated on axis) and elution of ^{125}I by γ-counting of each 500 μL fraction (●). Shown is the HPLC elution profile for the T-3 tryptic fragment of V8−25.

reverse-phase HPLC. The HPLC elution profile for the V8−12 fragment contains a single peak of ^{125}I counts per minute and a corresponding peak of absorbance, and fractions 34−37 were pooled and sequenced. For the V8−6 fragment, two peaks of ^{125}I counts per minute were evident in the HPLC elution profile and fractions 34−37 (V8−6A) and 39 and 40 (V8−6B) were pooled for sequence analysis. Finally, the single peak of ^{125}I counts per minute in the elution profile of V8−4 was pooled (fractions 34−36) and sequenced. Sequence analysis of fragments V8−12, V8−6A, and V8−4 revealed in each case the presence of a primary peptide beginning at Ile^{71} with predicted C-termini at Glu^{176}, Asp^{123}, and Asp^{123}, respectively (Table 3). As shown in Figure 9, fragments V8−4 and V8−6A each contain transmembrane segment M1, while the larger V8−12 fragment contains both the M1 and M2 segments. Transmembrane segment M3 was found to be present in the V8−6B fragment (amino terminus, Val^{279}; carboxy terminus, Glu^{319}; Table 3). The results of mapping the sites of [^{125}I]TIDPC/16 labeling in V8−15 indicate that membrane-spanning segments M1 and M3 are each exposed to the lipid bilayer, while segments M2 and M4 have no contact or limited contact with lipid (Figure 9).

From the amount of ^{125}I counts per minute and the intial yield determined from sequence analysis, the specific activities for each fragment were calculated: T-6 (V8−25), 205 cpm/pmol; T-3A (V8−25), 10 cpm/pmol; T-3B (V8−25), 274 cpm/pmol; V8−12 (V8−15), 123 cpm/pmol; V8−6A (V8−15), 65 cpm/pmol; V8−6B (V8−15), 8.3 cpm/pmol; and V8−4 (V8−15), 102 cpm/pmol.

DISCUSSION

Lipid-Exposed Transmembrane Segments of the Na,K-ATPase α-Subunit. The intent of this study was to employ lipophilic photoreactive probes to identify membrane-spanning segments of the Na,K-ATPase which are in contact with lipid as well as to monitor conformationally dependent movements in the transmembrane domain. The results provided here demonstrate that transmembrane segments M1, M3, M9, and M10 of the *Torpedo* Na,K-ATPase α-subunit are in contact with lipid and that collectively these segments likely constitute the bulk of the lipid−protein interface of the Na,K-ATPase. Evidence of conformationally dependent movements of transmembrane segments M5 and M6 is also provided, and these results are discussed in more detail in a later section.

Lipid exposure for segments of the Na,K-ATPase was demonstrated by first tagging lipid-exposed residues in transmembrane segments of the intact membrane-bound ATPase using the hydrophobic photoreagent 3-(trifluoromethyl)-3-(*m*-[^{125}I]iodophenyl)diazirine ([^{125}I]TID; Figure 1) and the phosphatidylcholine analogue [^{125}I]TIDPC/16 (Figure 6). Labeled peptide fragments were then isolated from proteolytic digests of the Na,K-ATPase α-subunit and the peptides identified by amino-terminal sequence analysis (Table 3 and Figure 9). Consistent with the hydrophobic nature of [^{125}I]TID as well as studies identifying the sites of labeling in other membrane proteins (see refs *24*, *25*, and *27* and references therein), the vast majority of [^{125}I]TID labeling in the Na,K-ATPase α-subunit maps to the same regions labeled by the photoreactive phospholipid [^{125}I]-TIDPC/16 and therefore represents labeling of lipid-exposed regions (Figures 5 and 8). Using [^{125}I]TIDPC/16, these lipid-

Table 3: Identification of [^{125}I]TIDPC/16-Labeled Fragments Produced by Further Proteolytic Digestion of Na,K-ATPase α-Subunit V8 Protease Fragments V8−25, V8−14, and V8−15[a]

fragment	apparent molecular mass (kDa)	N-terminal sequence (pmol of residue/cycle)	starting residue	predicted carboxy terminus (transmembrane segments)
T-6 (V8−25,−14)	6	N(6.2)S(4.1)I(14.9)F(10.1)Q(4.2)	N^{941}	R^{1004} (M9 and M10)
T-3A (V8−25,−14)	3	M(255)Y(303)P(153)L(301)K(195)	M^{979}	R^{1004} (M10)
T-3B (V8−25,−14)	3	N(ND)S(10.1)I(19.4)F(10.7)Q(6.6)	N^{941}	R^{978} (M9)
V8−12 (V8−15)	12	I(12)L(10.2)A(4.2)R(3.8)D(5.5)	I^{71}	E^{176} (M1 and M2)
V8−6A (V8−15)	6	I(25.7)L(30.3)A(28.6)R(12.5)D(32.8)	I^{71}	D^{123} (M1)
V8−6B (V8−15)	6	V(176)G(167)Q(130)T(89)P(66)	V^{279}	E^{319} (M3)
V8−4 (V8−15)	4	I(10.5)L(14.3)A(9.7)R(8.2)D(8.3)	I^{71}	D^{123} (M1)

[a] Apparent molecular mass values are those estimated from the electrophoretic mobility on 16.5% acrylamide Tricine SDS−PAGE gels (Figure 8). The parent fragment for each fragment resulting from further digestion is indicated by brackets. For fragments T-3 and V8−6, two peaks of ^{125}I counts per minute were evident in the reverse-phase HPLC profile. HPLC fractions 33−35 were pooled for T-3A, fractions 37−40 for T-3B, fractions 34−37 for V8−6A, and fractions 39 and 40 for V8−6B. The sequence of each fragment was identified within the primary structure of the *T. californica* Na,K-ATPase α-subunit (*29*).

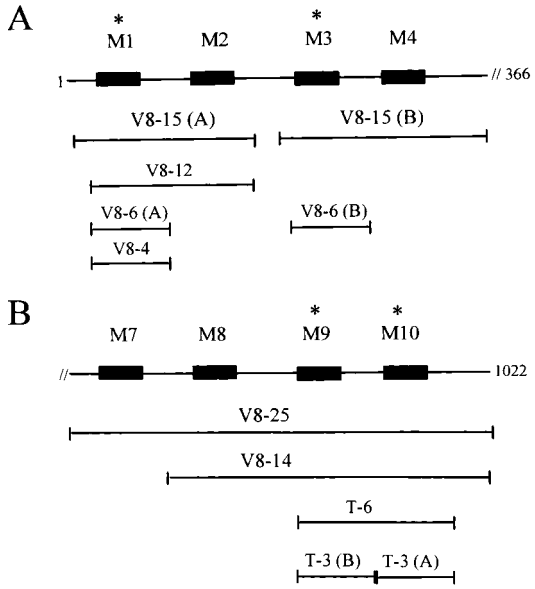

FIGURE 9: Map of [^{125}I]TIDPC/16-labeled proteolytic fragments in relation to the *Torpedo* Na,K-ATPase α-subunit sequence. The [^{125}I]TIDPC/16-labeled V8 protease fragments of the Na,K-ATPase α-subunit (V8−25, V8−14, and V8−15; Table 2) were further enzymatically digested and the resulting fragments isolated (Figure 8) and subjected to automated N-terminal protein sequencing. Using the amino acids detected in the first 5−10 cycles of protein sequencing, the position of each fragment in relation to the primary structure of the intact *T. californica* Na,K-ATPase α-subunit (*29*) was determined (Table 3). On the basis of the apparent molecular mass of each fragment and the known cleavage specificity of trypsin and V8 protease, the carboxy terminus of each fragment was predicted. (A) The approximate locations of the membrane-spanning domains (M1−M4) of the Na,K-ATPase α-subunit are shown. The amino acid stretch and transmembrane segments contained within intact V8 protease fragments V8−15A and V8−15B as well as fragments generated by further enzymatic digestion of these fragments are marked by brackets and named in accordance with their apparent molecular mass on a Tricine SDS−PAGE gel. (B) The corresponding map of the fragments generated from tryptic digestion of V8−25 and V8−14 is shown. In both maps, the asterisks indicate which transmembrane segments are labeled with [^{125}I]TIDPC/16 and therefore exposed to the lipid bilayer.

exposed regions were then further mapped. The fact that the principal [^{125}I]TIDPC/16-labeled proteolytic fragments were shown to contain transmembrane segments M1, M3, M9, and M10 (Figure 9) indicates that these segments have the greatest levels of exposure to the lipid bilayer and therefore likely constitute the bulk of the lipid−protein interface of the Na,K-ATPase α-subunit. The fact that no [^{125}I]TIDPC/16-labeled fragments were identified (e.g., Figure 8 and Table 3) which contain transmembrane segments M2 and M4−M8 indicates that neither of these transmembrane segments is in contact with lipid or that their exposure to the lipid bilayer is substantially limited. The extent of [^{125}I]TID and [^{125}I]TIDPC/16 photoincorporation into proteolytic fragments containing the M1, M3, M9, and M10 segments (V8−25, −15, and −14) is the same whether the fragments are isolated from ATPase labeled in the E_1 or E_2 conformation (Figure 4). These results indicate that the transmembrane segments of the Na,K-ATPase α-subunit which lie at the lipid−protein interface do not undergo any detectable conformationally dependent movements, or at least movements of sufficient magnitude to affect the exposure of these segments to the lipid bilayer. However, it remains possible that these lipid-exposed transmembrane segments do undergo small conformationally dependent movements or, perhaps less likely, that there are movements of substantial magnitude but which lead to compensatory amounts of surface area that is exposed to the lipid bilayer and therefore lead to no detectable changes in the extent of [^{125}I]TIDPC/16 labeling. Additional studies are presently underway to identify individual lipid-exposed amino acids in each of these transmembrane segments, and the results of these studies should provide further insight into any possible conformationally dependent movements of transmembrane segments at the Na,K-ATPase lipid−protein interface. Interestingly, in a recent report Stokes and colleagues (*30*), they compared the 8 Å structures of the Ca^{2+}-ATPase and H^+-ATPase and found that the arrangement of transmembrane segments was remarkably similar in the two molecules. This was despite the fact that sequence similarities in the membrane-spanning segments of each of these two ATPase are rather limited and that the structure of the Ca^{2+}-ATPase was determined in the E_2 conformation and that of the H^+-ATPase in the E_1 conformation. The authors interpreted these results as suggesting that small rearrangements of the transmembrane segments of P-type ion-motive ATPases take place during cation transport. The results of our study showing that there are no detectable movements in the transmembrane segments at the lipid−protein interface of the homologous Na,K-ATPase are consistent with this conclusion.

Structural Transitions of the Transmembrane Segments of the Na,K-ATPase α-Subunit. As was discussed in the

preceding section, the results of recent studies, including the present study, suggest that cation transport in the Na,K-ATPase as well as in other members of the P-type ion-motive ATPase family is accomplished by small movements of the transmembrane segments. The results of [^{125}I]TID photoincorporation into the Na,K-ATPase α-subunit provide additional insight into these transmembrane structural transitions. For [^{125}I]TID, there was more extensive labeling of the Na,K-ATPase α-subunit in the E_2 conformation than in the E_1 conformation (Figure 2). The enhanced [^{125}I]TID labeling in the E_2 conformation was subsequently mapped to fragments which contain transmembrane segments M5 and M6 (Figures 3 and 4 and Table 1). Given the extensive data implicating residues in the M5 and M6 (as well as M4 and M8) transmembrane segments as being important for cation occlusion and cation transport (reviewed in ref *12*), the obvious possibility is that [^{125}I]TID is binding within the cation transport pathway and reporting conformationally dependent changes in the structure of the pathway. Along these lines, TID is a weak inhibitor of the *Torpedo* Na,K-ATPase, inhibiting ATPase activity in a concentration-dependent manner with an IC_{50} value of 500 μM (data not shown). There are then two components to the photoincorporation of TID into the Na,K-ATPase: (1) a conformationally sensitive component reflecting labeling of amino acids in the M5 and M6 segments, residues which may contribute to the cation translocation pathway, and (2) a conformationally insensitive component which maps to transmembrane segments also labeled by the photoreactive phospholipid [^{125}I]TIDPC/16 and which are located at the lipid−protein interface of the Na,K-ATPase α-subunit. In studies which extensively characterized the sites of [^{125}I]TID photoincorporation into the subunits of the nicotinic acetylcholine receptor (AChR), a completely analogous result was found. First, TID is a potent noncompetitive antagonist of the AChR, and one component of [^{125}I]TID photoincorporation which is sensitive to the conformational state of the receptor is localized to the channel-lining M2 segments of each receptor subunit (*22*, *23*, *26*). In addition, [^{125}I]TID also photoincorporates in a conformationally insensitive manner into amino acids in the M1, M3, and M4 transmembrane segments of each receptor subunit, reflecting labeling of residues situated at the lipid−protein interface of the AChR (*24*, *25*).

An alternative possibility is that the difference in the extent of [^{125}I]TID photoincorporation into the M5 and M6 segments of the Na,K-ATPase α-subunit is a reflection of a conformationally dependent change in the exposure of these segments to the lipid bilayer. This possibility is rendered unlikely due to the fact that the photoreactive phospholipid [^{125}I]TIDPC/16 does not label the M5 and M6 transmembrane segments in either conformation, indicating that these segments are not exposed to lipid in either the E_1 or E_2 conformation. Another possibility is that [^{125}I]TID may not bind within the actual pathway traversed by cations but rather may bind within a pocket formed between the transmembrane segments of the Na,K-ATPase α-subunit, with the pocket lined at least in part by the M5 and M6 segments. In this scenario, the change in the extent of [^{125}I]TID photoincorporation into the M5 and M6 segments in the E_1 and E_2 conformations would reflect a conformationally dependent change in the structure of that transmembrane pocket. Studies which lead to the identification of amino acids that react with [^{125}I]TID in the M5 and M6 segments in the E_1 and E_2 conformations of the Na,K-ATPase will undoubtedly resolve this issue as well as lead to potentially important insights into the structural transitions that occur in the transmembrane domain during cation transport.

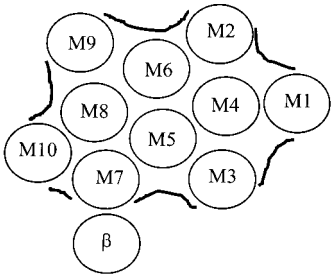

FIGURE 10: Model of the spatial organization of membrane-spanning segments in the Na,K-ATPase. The model is based on the spatial arrangement of transmembrane α-helices determined for the sarcoplasmic reticulum Ca^{2+}-ATPase (*6*) and has been expanded to include the positioning of the single transmembrane segment of the Na,K-ATPase β-subunit in proximity to the M7 membrane-spanning segment.

Spatial Organization of Transmembrane Segments of the Na,K-ATPase α-Subunit. Figure 10 presents a model of the spatial arrangements of transmembrane segments of the Na,K-ATPase. The arrangement is based on the determined arrangement of transmembrane α-helices in the recently published crystal structure (2.6 Å resolution) of the sarcoplasmic reticulum Ca^{2+}-ATPase. (*6*). The results of our study with the Na,K-ATPase are largely consistent with the arrangement of transmembrane α-helices in the Ca^{2+}-ATPase and to varying degrees inconsistent with previously proposed models for the Na,K-ATPase (*9*, *28*). In the Na,K-ATPase α-subunit, transmembrane segments M1, M3, M9, and M10 are the principal sites of labeling of the photoreactive phospholipid [^{125}I]TIDPC/16 and therefore are interpreted as constituting the bulk of the lipid−protein interface. In agreement with the photolabeling data, in the Ca^{2+}-ATPase (Figure 10) the corresponding homologous transmembrane α-helical segments are each located at the periphery of the transmembrane complex with each segment exhibiting substantial exposure to the lipid bilayer. In the Ca^{2+}-ATPase, segments M4−M6 and M8 are positioned toward the interior of the complex, which is in line with the role that these segments play in cation binding and translocation. The lack of [^{125}I]TIDPC/16 labeling into Na,K-ATPase α-subunit fragments which contain each of these segments indicates that these segments exhibit little or no exposure to the lipid bilayer, which is consistent with the Na,K-ATPase and Ca^{2+}-ATPase having homologous transmembrane structures. Two notable exceptions between the photolabeling results with the Na,K-ATPase and the transmembrane structure of the Ca^{2+}-ATPase are that in the calcium pump transmembrane segments M7 and M2 are located near the periphery of the transmembrane complex with substantial exposure to the lipid bilayer. In contrast, no [^{125}I]TIDPC/16-labeled fragment was identified containing either the M7 or M2 segment of the Na,K-ATPase, suggesting that these two segments have no exposure or limited exposure to the lipid bilayer. These results may indicate that the spatial organization of transmembrane segments in the Na,K-ATPase and Ca^{2+}-ATPase

are different, as suggested by models derived in part by chemical cross-linking experiments (*9*). One alternative possibility is that in the Na,K-ATPase the single transmembrane segment of the β-subunit may be localized next to the M7 segment where it could prevent [^{125}I]TIDPC/16 labeling of residues in M7 (Figure 10). In agreement with the positioning of the β-subunit next to M7 are cross-linking studies, studies which examined which proteolytic fragments copurify with the β-subunit of the H^+-ATPase, as well as other studies (*9*, *31*) that all suggest that the β-subunit associates with the region of the α-subunit containing transmembrane segments M7 and M8. However, the above-mentioned cross-linking studies also support the alternative positioning of the transmembrane segment of the β-subunit next to M8. Finally, an additional possibility is that in the proposed diprotomeric ATPase complex $(\alpha\beta)_2$ (*1*), the association involves the M2 segments of each α-subunit. The association of the two transmembrane M2 segments would then prevent exposure of these segments to [^{125}I]TIDPC/16 from the lipid bilayer. Clearly, additional studies are needed to further define the spatial arrangement of transmembrane segments in the Na,K-ATPase. Studies aimed at identifying lipid-exposed transmembrane segments in other P-type ion-motive ATPases, including the Ca^{2+}-ATPase (SERCA1), are also currently underway. The results of these studies will likely provide additional insight into the spatial arrangement of transmembrane segments in P-type ion-motive ATPases in general as well as with regard to the lipid exposure of the M2 and M7 transmembrane segments in the Na,K-ATPase.

ACKNOWLEDGMENT

We thank Dr. Josef Brunner (Swiss Federal Institute of Technology Zurich) for kindly providing the tin precursor TTDPC/16.

REFERENCES

1. Vasilets, L. A., and Schwarz, W. (1993) *Biochim. Biophys. Acta 1154*, 201−222.
2. Stokes, D. L., Taylor, W. R., and Green, N. M. (1994) *FEBS Lett. 346*, 32−38.
3. MacLennan, D. H., Rice, W. J., and Green, N. M. (1997) *J. Biol. Chem. 272*, 28815−28818.
4. Scarborough, G. A. (2000) *J. Exp. Biol. 203*, 147−154.
5. Moller, J. V., Juul, B., and LeMaire, M. (1996) *Biochim. Biophys. Acta 1286*, 1−51.
6. Toyoshima, C., Nakasako, M., Nomura, H., and Ogawa, H. (2000) *Nature 405*, 647−655.
7. Auer, M., Scarborough, G. A., and Kuhlbrandt, W. (1998) *Nature 392*, 840−843.
8. Taylor, K. A., and Varga, S. (1994) *J. Biol. Chem. 269*, 10107−10111.
9. Or, E., Goldshleger, R., and Karlish, S. J. D. (1999) *J. Biol. Chem. 274*, 2802−2809.
10. Karlish, S. J. D., Goldshleger, R., and Stein, W. D. (1990) *Proc. Natl. Acad. Sci. U.S.A. 87*, 4566−4570.
11. Capasso, J. M., Hoving, S., Tal, D. M., Goldshleger, R., and Karlish, S. J. D. (1992) *J. Biol. Chem. 267*, 1150−1158.
12. Nielsen, J. M., Pedersen, P. A., Karlish, S. J. D., and Jorgensen, P. L. (1998) *Biochemistry 37*, 1961−1968.
13. Blanton, M. P., McCardy, E. A., Huggins, A., and Parikh, D. (1998) *Biochemistry 37*, 14545−14555.
14. Sobel, A., Weber, M., and Changeux, J. P. (1977) *Eur. J. Biochem. 80*, 215−224.
15. Pedersen, S. E., Dreyer, E. B., and Cohen, J. B. (1986) *J. Biol. Chem. 261*, 13735−13743.
16. Pressley, T. A., Haber, R. S., Loeb, J. N., Edelman, I. S., and Ismail-Beigi, F. (1986) *J. Gen. Physiol. 87*, 591−606.
17. Lowry, O. H., Rosebrough, N. S., Farr, A. L., and Randall, R. J. (1951) *J. Biol. Chem. 193*, 265−275.
18. Heimburg, T., Esmann, M., and Marsh, D. (1997) *J. Biol. Chem. 272*, 25685−25692.
19. Laemmli, U. K. (1970) *Nature 227*, 680−685.
20. Cleveland, D. W., Fischer, S. G., Kirschner, M. W., and Laemmli, U. K. (1977) *J. Biol. Chem. 252*, 1102−1106.
21. Schagger, H., and von Jagow, G. (1987) *Anal. Biochem. 166*, 368−379.
22. White, B. H., Howard, S., Cohen, S. G., and Cohen, J. B. (1991) *J. Biol. Chem. 266*, 21595−21607.
23. White, B. H., and Cohen, J. B. (1992) *J. Biol. Chem. 267*, 15770−15783.
24. Blanton, M. P., and Cohen, J. B. (1992) *Biochemistry 31*, 3738−3750.
25. Blanton, M. P., and Cohen, J. B. (1994) *Biochemistry 33*, 2859−2872.
26. Blanton, M. P., McCardy, E. A., and Gallagher, M. J. (2000) *J. Biol. Chem. 275*, 3469−3478.
27. Brunner, J. (1993) *Annu. Rev. Biochem. 62*, 483−514.
28. Modyanov, N., Lutsenko, S., Chertova, E., Efremov, C. R., and Gulyaev, D. (1992) *Acta Physiol. Scand. 146*, 49−58.
29. Kawakami, K., Noguchi, S., Noda, M., Takahashi, H., Ohta, T., Kawamura, M., Nojima, H., Nagano, K., Hirose, T., Inayama, S., Hayashida, H., Miyata, T., and Numa, S. (1985) *Nature 316*, 733−736.
30. Stokes, D. L., Auer, M., Zhang, P., and Kuhlbrandt, W. (1999) *Curr. Biol. 9*, 672−679.
31. Munson, K., Lambrecht, N., Shin, J. M., and Sachs, G. (2000) *J. Exp. Biol. 203*, 161−170.
32. Skou, J. C., and Esmann, M. (1980) *Biochim. Biophys. Acta. 601*, 386.

BI0015461